Spatial Modulation Using Signal Space Diversity

Mehmet Akif Kurt, *Student Member, IEEE*, Ali Tugberk Dogukan, *Student Member, IEEE*, and Ertugrul Basar, *Fellow, IEEE*

***Abstract*— In this letter, a novel scheme, called spatial modulation (SM) using signal space diversity (SM-SSD), is proposed for future multiple-input multiple-output (MIMO) systems. In this scheme, consecutive time slots are modulated jointly, and the technique of signal and space diversity (SSD) is applied to spread the real and imaginary parts of data symbols over the time domain. In addition, novel active antenna activation pattern and time activation pattern selection algorithms are introduced. An upper bound expression for bit error rate (BER) is obtained and a diversity analysis is performed. Besides, a suboptimal solution for the optimization of rotation angles is put forward to maximize the minimum coding gain distance (MCGD). Monte Carlo simulations are performed to compare the BER performance of SM-SSD with the benchmark schemes, in the presence of both correlated and uncorrelated channels. Lastly, the change in the spectral efficiency is analyzed for different numbers of time slots and transmit antennas.**

***Index Terms*— SM, index modulation, diversity gain, signal space diversity, minimum coding gain distance.**

I. Introduction

MULTIPLE-INPUT multiple-output (MIMO) systems are promising to satisfy the challenging requirements of the next-generation wireless technologies since these systems enable higher spectral and energy efficiencies. In recent years, index modulation (IM) has stood out as a novel approach for MIMO systems since it increases the spectral and energy efficiencies while minimizing the transceiver complexity [1], [2]. In the context of IM, space modulation techniques (SMTs) have been proposed to convey additional information bits in the spatial domain and have lower hardware and receiver complexities [3], [4], [5], [6]. Specifically, spatial modulation (SM) activates only one transmit antenna, which limits the spectral efficiency. To enhance the spectral efficiency and the bit error rate (BER) performance, generalized SM (GSM) and quadrature SM (QSM) are proposed [7], [8]. GSM conveys more information bits than SM by activating more than one transmit antenna and uses the transmit antennas efficiently. On the other hand, QSM activates one transmit antenna for the real and imaginary parts of data symbol separately. In this way, QSM doubles the number of the information bits sent through the spatial domain and decreases the modulation order. Capacity optimized antenna selection (COAS) and Euclidian distance antenna selection (EDAS) are transmit antenna selection (TAS) based SM schemes and intend to improve the BER performance by increasing the signal-to-noise ratio (SNR) and maximizing minimum Euclidian distance, respectively [9]. Space-time coding (STC) schemes activate multiple transmit antennas and modulate data symbols. In this way, STC schemes provide transmit diversity and improve the BER performance [10], [11], [12]. However, modulating more than one data symbol increases the required number of radio frequency (RF) chains. Thus, these schemes have higher hardware complexity at the transmitter side than SM schemes.

Signal space diversity (SSD) is a new diversity technique that interleaves the real and imaginary parts of data symbols for Rayleigh fading channels [13]. SSD is applied for SM-based transmission schemes to improve the BER performance through the transmit diversity enhancement and to decrease hardware complexity by using only one RF chain [14], [15]. In these schemes, data symbols are selected from rotated constellations. After that, the real and imaginary parts are transmitted over consecutive time slots. With this methodology, higher diversity orders are obtained with a single RF chain, which is one of the main properties of SM.

In this letter, a novel transmission scheme SM using signal space diversity (SM-SSD) is proposed for MIMO systems. SM-SSD uses the SSD technique and sends the data symbols over multiple time slots to increase transmit diversity compared to existing SM schemes. The proposed SM-SSD scheme is generalized for multiple successive time slots, which are modulated simultaneously, and uses the SSD technique to mix up the real and imaginary parts of data symbols in the time domain. A unique shifting mechanism is introduced to apply SSD, and it circularly shifts the imaginary parts of rotated data symbols in the time domain. The introduced time activation pattern (TAP) selection algorithm determines the placement of data symbols in the time domain for transmission according to the incoming bits, while the proposed antenna activation pattern (AAP) selection algorithm activates transmit antennas cleverly to guarantee a diversity order of 2. In the diversity analysis section, the worst-case scenarios for the transmitted and detected transmission matrices are analyzed, and it is shown that a diversity order of 2 is guaranteed thanks to our shifting mechanism, AAP, and TAP algorithms. Furthermore, similar to classical SM, SM-SSD requires only one RF chain, which significantly reduces the hardware complexity. After the system model of SM-SSD is introduced, the theoretical

Manuscript received 27 October 2022; revised 7 December 2022; accepted 29 December 2022. Date of publication 11 January 2023; date of current version 10 March 2023. The associate editor coordinating the review of this letter and approving it for publication was R. S. Kshetrimayum. *(Corresponding author: Ertugrul Basar.)*

The authors are with the Communications Research and Innovation Laboratory (CoreLab), Department of Electrical and Electronics Engineering, Koç University, Sariyer, 34450 Istanbul, Turkey (e-mail: mkurt20@ku.edu.tr; adogukan18@ku.edu.tr; ebasar@ku.edu.tr).

Digital Object Identifier 10.1109/LCOMM.2023.3236025

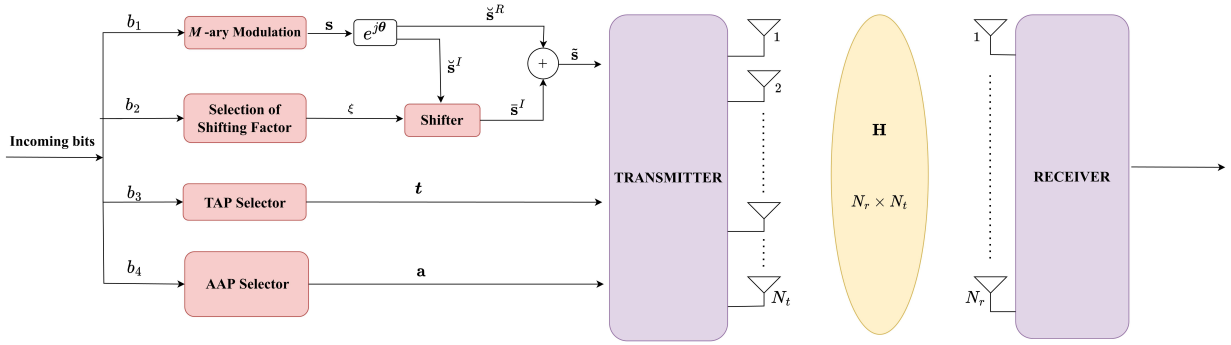

Fig. 1. SM-SSD System Model.

upper bound for the error performance is expressed. Besides, Monte Carlo simulations are demonstrated to compare the BER performance of SM-SSD with the benchmark schemes and to show that enhanced transmit diversity considerably improves the BER performance of SM-SSD. In addition, Monte Carlo simulations are also performed to show the validity of theoretical upper bound derivations and to observe the effect of correlated channels on the error performance.

II. System Model

We consider a MIMO configuration with N_t transmit and N_r receive antennas. A total number of b bits are transmitted over Ω successive time slots and these bits are split into four parts. Firstly, $b_1 = \Omega \log_2(M)$ bits determine Ω M-PSK/QAM modulated data symbols, $\mathbf{s} = [s_1, s_2, \cdots, s_\Omega]^{\mathrm{T}}$, where M and $(\cdot)^{\mathrm{T}}$ are the modulation order and transposition operator, respectively. The μ-th element of the data symbol vector is rotated with an angle θ_μ, $\breve{s}_\mu = s_\mu e^{j\theta_\mu}$, $\breve{\mathbf{s}} = [s_1 e^{j\theta_1}, s_2 e^{j\theta_2}, \cdots, s_\Omega e^{j\theta_\Omega}]^{\mathrm{T}}$, $\mu = 1, \cdots, \Omega$, and this rotated data symbol vector is separated into its real and imaginary parts as $\breve{\mathbf{s}}^R$ and $\breve{\mathbf{s}}^I$, where $\breve{\mathbf{s}} = \breve{\mathbf{s}}^R + j\breve{\mathbf{s}}^I$. Note that constellation rotation is a must in SSD-based schemes to provide a diversity gain [13]. In addition, the rotation of data symbols does not cause an additional computational complexity since it involves simple multiplication. Secondly, in order to apply SSD, $b_2 = \lfloor \log_2(\Omega - 1) \rfloor$ bits decide a shifting factor ξ to shift the vector $\breve{\mathbf{s}}^I$ circularly and its circularly shifted version is expressed as $\bar{\mathbf{s}}^I = [\bar{s}_1^I, \bar{s}_2^I, \cdots, \bar{s}_\Omega^I]^{\mathrm{T}}$, where $\bar{\mathbf{s}}_k^I = \breve{\mathbf{s}}_i^I$, $\xi \in \{1, \cdots, \Omega - 1\}$, $k = \mathrm{mod}(i - \xi, \Omega)$ if $\mathrm{mod}(i - \xi, \Omega) > 0$ and $k = \Omega$ if $\mathrm{mod}(i - \xi, \Omega) = 0$, $i, k \in \{1, \cdots, \Omega\}$ where mod is the modulo operator. Then, the new data symbol vector is obtained as $\tilde{\mathbf{s}} = \breve{\mathbf{s}}^R + j\bar{\mathbf{s}}^I = [\tilde{s}_1, \tilde{s}_2, \cdots, \tilde{s}_\Omega]^{\mathrm{T}}$. Hence, the real and imaginary parts of each data symbol are transmitted over different time slots. Thirdly, $b_3 = \lfloor \log_2(\Omega!) \rfloor$ bits select the time slot activation pattern (TAP), $\mathbf{t} = [t_1, t_2, \cdots, t_\Omega]^{\mathrm{T}}$, $t_\mu \in \{1, 2, \cdots, \Omega\}$. Fourthly, $b_4 = \lfloor \log_2(N_t) \rfloor$ bits specify the antenna activation pattern (AAP), $\mathbf{a} = [a_1, a_2, \cdots, a_\Omega]^{\mathrm{T}}$. The method for the generation of TAPs and AAPs is discussed in the sequel. Finally, the μ-th data symbol $(\tilde{\mathbf{s}}_\mu)$ is transmitted in time slot t_μ from the a_μ-th transmit antenna. The transmitted vector $\mathbf{x}^{(t_\mu)} \in \mathbb{C}^{N_t \times 1}$ at time slot t_μ can be shown as:

$$\mathbf{x}^{(t_\mu)} = [0, \cdots, \underbrace{\tilde{s}_\mu}_{a_\mu}, \cdots, 0]^{\mathrm{T}}. \tag{1}$$

TABLE I

Shifting Mechanism of $\breve{\mathbf{s}}^I$ According to b_2 Bits for $\Omega = 3$

b_2 bits	ξ	$\bar{\mathbf{s}}^I$
$\{0\}$	1	$[\breve{s}_3^I \breve{s}_1^I \breve{s}_2^I]^{\mathrm{T}}$
$\{1\}$	2	$[\breve{s}_2^I \breve{s}_3^I \breve{s}_1^I]^{\mathrm{T}}$

TABLE II

TAP Selection According to b_3 Bits for $\Omega = 3$

b_3 bits	TAP $(\mathbf{t})$
$\{00\}$	$[1, 2, 3]^{\mathrm{T}}$
$\{01\}$	$[1, 3, 2]^{\mathrm{T}}$
$\{10\}$	$[2, 1, 3]^{\mathrm{T}}$
$\{11\}$	$[2, 3, 1]^{\mathrm{T}}$

Therefore, the transmission matrix is given as $\mathbf{X} = [\mathbf{x}^{(1)}, \cdots, \mathbf{x}^{(\Omega)}] \in \mathbb{C}^{N_t \times \Omega}$, whose t_μ-th column represents $\mathbf{x}^{(t_\mu)}$.

The spectral efficiency of the proposed scheme in bits per channel use (bpcu) can be given as:

$$\eta = \frac{\Omega \log_2(M) + \lfloor \log_2(\Omega - 1) \rfloor + \lfloor \log_2(\Omega!) \rfloor + \lfloor \log_2(N_t) \rfloor}{\Omega}. \tag{2}$$

Remark 1 (TAPs Creation): Since the length of a TAP is Ω, the total number of all possible TAPs is $\Omega!$ by permutation. Thus, the set, which includes all possible TAPs, is given as $\mathcal{G} = \{\mathbf{t}_1, \cdots, \mathbf{t}_{\Omega!}\}$, $\mathbf{t}_g = [t_{g,1}, \cdots, t_{g,\Omega}]^{\mathrm{T}}$, $g = 1, \cdots, \Omega!$. For example, assuming $\Omega = 3$, this set is expressed as follows:

$$\mathcal{G} = \left\{ \begin{bmatrix} 1 \\ 2 \\ 3 \end{bmatrix}, \begin{bmatrix} 1 \\ 3 \\ 2 \end{bmatrix}, \begin{bmatrix} 2 \\ 1 \\ 3 \end{bmatrix}, \begin{bmatrix} 2 \\ 3 \\ 1 \end{bmatrix}, \begin{bmatrix} 3 \\ 1 \\ 2 \end{bmatrix}, \begin{bmatrix} 3 \\ 2 \\ 1 \end{bmatrix} \right\}. \tag{3}$$

Only $2^{\lfloor \log_2(\Omega!) \rfloor}$ out of $\Omega!$ possible TAPs can be utilized to transmit $\lfloor \log_2(\Omega!) \rfloor$ number of information bits by the indices of TAPs. In this study, we employ the first $2^{\lfloor \log_2(\Omega!) \rfloor}$ TAPs.

Remark 2 (AAPs Creation): Here, we propose a clever AAP selection strategy. This strategy is valid only for $N_t \geq \Omega$ since it activates different transmit antennas in each time slots. Let us define a set $\mathcal{A} = \{\mathbf{a}_1, \cdots, \mathbf{a}_{N_t}\}$, which includes all possible AAPs. The ν-th AAP is defined as

$$\mathbf{a}_\nu = [\mathrm{mod}(\nu, N_t), \mathrm{mod}(\nu + 1, N_t), \cdots, \mathrm{mod}(\nu + \Omega - 1, N_t)]^{\mathrm{T}}. \tag{4}$$

If any element of $\mathbf{a}_\nu$ is equal to 0, its value is changed as N_t. For instance, assuming $N_t = 4$ and $\Omega = 3$, the set including

all possible AAPs is given by

$$\mathcal{A} = \left\{ \begin{bmatrix}1\\2\\3\end{bmatrix}, \begin{bmatrix}2\\3\\4\end{bmatrix}, \begin{bmatrix}3\\4\\1\end{bmatrix}, \begin{bmatrix}4\\1\\2\end{bmatrix} \right\}. \quad (5)$$

Note that AAP and TAP algorithms do not increase the computational complexity because no complex calculation is performed.

The received signal $\mathbf{y} \in \mathbb{C}^{N_R \mathrm{x} 1}$ at the receiver is given by $\mathbf{y} = \sqrt{\rho}\mathbf{H}\mathbf{x} + \mathbf{n}$, where $\mathbf{H} \in \mathbb{C}^{N_r \mathrm{x} N_t}$ is a Rayleigh fading channel matrix whose entries independent and identically distributed complex Gaussian random variables with $\mathcal{CN}(0,1)$ distribution and $\mathbf{n} \in \mathbb{C}^{N_t \mathrm{x} 1}$ is an additive white Gaussian noise vector whose entries are independent and identically distributed complex Gaussian random variables with $\mathcal{CN}(0,1)$. ρ is average signal-to-noise ratio at each receiver antenna. At the receiver, indices of activated transmit antennas and data symbols are determined using maximum likelihood (ML) detector. ML detector is applied for Ω consecutive time slots and it works as follows

$$[\hat{\xi}, \hat{\mathbf{a}}, \hat{\mathbf{t}}, \hat{\mathbf{s}}] = \arg\min_{\xi, \mathbf{a}, \mathbf{t}, \mathbf{s}} \sum_{n=1}^{\Omega} ||\mathbf{y}^{(n)} - \sqrt{\rho}\mathbf{H}^{(n)}\mathbf{x}^{(n)}||^2, \quad (6)$$

where $\mathbf{y}^{(n)}$, $\mathbf{H}^{(n)}$ are the received signal vector and the channel matrix for the corresponding n-th time slot, respectively. In (6), $\hat{\xi}$, $\hat{\mathbf{a}}$, $\hat{\mathbf{t}}$ and $\hat{\mathbf{s}}$ stand for the detected shifting factor, AAP, TAP and the data symbol vector, respectively. Here, an ML detector makes an exhaustive search over all possible transmission matrices, thus, the number of ML metric calculations in (6) is $\Omega\eta$.

III. Performance Analysis

In this section, the theoretical analysis of the BER performance of SM-SSD, and optimization of its rotation angles are presented. In addition, a diversity analysis and correlated channels are discussed.

A. Theoretical Analysis and BER Optimization

In this subsection, firstly, we obtain an upper bound on the BER of SM-SSD system under the assumption of ML detection. As in [16], an upper bound on the BER of SM-SSD can be obtained as:

$$P_b \leq \frac{1}{(\Omega\eta)2^{(\Omega\eta)}} \sum_{\omega=1}^{2^{(\Omega\eta)}} \sum_{\phi=1}^{2^{(\Omega\eta)}} P(\mathbf{X}_\omega \rightarrow \hat{\mathbf{X}}_\phi) e(\mathbf{X}_\omega, \hat{\mathbf{X}}_\phi). \quad (7)$$

In (7), $P(\mathbf{X}_\omega \rightarrow \hat{\mathbf{X}}_\phi)$ and $e(\mathbf{X}_\omega, \hat{\mathbf{X}}_\phi)$ are pairwise error probability (PEP) and the number of erroneous bits, respectively, when $\mathbf{X}_\omega$ is transmitted and $\hat{\mathbf{X}}_\phi$ is incorrectly detected. For the proposed scheme, the conditional pairwise error probability (CPEP) can be expressed as $P(\mathbf{X}_\omega \rightarrow \hat{\mathbf{X}}_\phi|\mathbf{H}) = Q\left(\sqrt{\frac{\rho||(\mathbf{X}_\omega - \hat{\mathbf{X}}_\phi)\mathbf{H}||^2}{2}}\right)$ where $Q(x) = \frac{1}{\pi}\int_0^{\frac{\pi}{2}} \exp(\frac{-x^2}{\sin^2\theta})\, d\theta$. PEP can be expressed as in (8) by taking the average of CPEP over $\mathbf{H}$ using moment generating function (MGF):

$$P(\mathbf{X}_\omega \rightarrow \hat{\mathbf{X}}_\phi) = \frac{1}{\pi}\int_0^{\frac{\pi}{2}} \kappa^{(1)}(\gamma)\kappa^{(2)}(\gamma)\ldots\kappa^{(\Omega)}(\gamma) d\gamma. \quad (8)$$

where $\kappa^{(\chi)}(\gamma) = \left(\frac{\sin^2\gamma}{\sin^2\gamma + \frac{\rho\lambda_\chi}{4}}\right)^{N_r}$, and $\lambda_\chi, \chi = 1, 2, \ldots, \Omega$ are the eigenvalues of $\mathbf{A}$, where $\mathbf{A} = (\mathbf{X}_\omega - \hat{\mathbf{X}}_\phi)^H(\mathbf{X}_\omega - \hat{\mathbf{X}}_\phi)$ is the difference matrix.

The BER performance of SM-SSD are dictated by the rotation vector $\boldsymbol{\theta}$. An exhaustive search for all elements of $\boldsymbol{\theta}$ is not efficient and due to this, we propose a suboptimal solution and define the elements of $\boldsymbol{\theta}$ depending on θ'. Since quadrature amplitude modulation (QAM) constellation repeats itself in every 90^o, the μ-th element of $\boldsymbol{\theta}$ can be obtained as $\theta_\mu = \theta' + 90(\mu - 1)/\Omega$. To determine the optimal θ' value, the minimum coding gain distance (MCGD) is considered as in [17]. MCGD is calculated as $\delta_{\min} = \min_{\mathbf{X}, \hat{\mathbf{X}}} det(\mathbf{A})$.

The optimal θ' can be expressed as $(\theta'_{\text{opt}}) = \arg\max_{\theta'} \delta_{\min}$. The maximum MCGD values are observed at $\theta'_{opt} = 11^o$ and $\theta'_{opt} = 18^o$ for 4-QAM and 8-QAM, respectively. Then, $\theta'_{opt} = 11^o$ and $\theta'_{opt} = 18^o$ are selected as suboptimal rotation angles for 4-QAM and 8-QAM, respectively.

To observe the effect of correlation between the channels, the Kronecker model is considered [18]. Accordingly, the correlated channel matrix can be expressed as $\mathbf{H}_{corr} = \mathbf{R}_L^{1/2}\mathbf{H}\mathbf{R}_R^{1/2}$ where $\mathbf{R}_L^{1/2} \in \mathbb{C}^{N_r \mathrm{x} N_r}$ and $\mathbf{R}_R^{1/2} \in \mathbb{C}^{N_t \mathrm{x} N_t}$ are spatial correlation matrices at the transmitter and the receiver, respectively. The entries of the spatial correlation matrices are $\mathbf{R}_{L,i,j}^{1/2} = \mathbf{R}_{R,i,j}^{1/2} = \tau^{-|i-j|}$ where τ is the correlation coefficient.

B. Diversity Analysis

In this section, we investigate the worst case pairwise error events to give insight on the diversity order of the proposed scheme.

1) Symbol Selection: We first investigate the effect of data symbol selection on the diversity order. Assume that the transmission matrix $\mathbf{X}$, with parameters $N_t = 4$, $\Omega = 3$, $\xi = 1$, $\mathbf{t} = [1, 3, 2]^{\mathrm{T}}$, $\mathbf{a} = [2, 3, 4]^{\mathrm{T}}$, $\breve{\mathbf{s}} = [\breve{s}_1, \breve{s}_2, \breve{s}_3]^{\mathrm{T}}$, is transmitted, and $\hat{\mathbf{X}}$ is erroneously detected only with a single symbol error ($\breve{s}_1 \rightarrow \breve{s}_{e,1}$) while shifting factor, TAP, and AAP are decoded correctly. In this case, the corresponding error event can be expressed as follows:

$$\mathbf{X} \rightarrow \hat{\mathbf{X}} = \begin{bmatrix} 0 & 0 & 0 \\ \breve{s}_1^R + j\breve{s}_3^I & 0 & 0 \\ 0 & \breve{s}_3^R + j\breve{s}_2^I & 0 \\ 0 & 0 & \breve{s}_2^R + j\breve{s}_1^I \end{bmatrix} \rightarrow \begin{bmatrix} 0 & 0 & 0 \\ \breve{s}_{e,1}^R + j\breve{s}_3^I & 0 & 0 \\ 0 & \breve{s}_3^R + j\breve{s}_2^I & 0 \\ 0 & 0 & \breve{s}_2^R + j\breve{s}_{e,1}^I \end{bmatrix}. \quad (9)$$

For this specific error event, $\mathbf{A} = (\mathbf{X} - \hat{\mathbf{X}})^{\mathrm{H}}(\mathbf{X} - \hat{\mathbf{X}})$ is calculated, where $\mathrm{rank}(\mathbf{A}) = d_1 = 2$ represents the diversity order. This can be explained by the fact that one symbol error results in two non-zero elements, which are located in different rows and columns, in $\mathbf{A}$. Hence, in $\mathbf{A}$, we can have at least 2 linearly independent rows or columns, which guarantees a diversity order of 2. We note that this is the worst case error event. If more than one symbol error occurs, a diversity order higher than 2 is always obtained.

2) Shifting Factor Selection: Secondly, the effect of shifting factor error on the diversity order is examined. Assume that the transmission matrix $\mathbf{X}$, with parameters $N_t = 4$, $\Omega = 3$, $\xi = 1$, $\mathbf{t} = [1,3,2]^{\mathrm{T}}$, $\mathbf{a} = [2,3,4]^{\mathrm{T}}$, $\breve{\mathbf{s}} = [\breve{s}_1, \breve{s}_2, \breve{s}_3]^{\mathrm{T}}$, is transmitted, and $\hat{\mathbf{X}}$ is erroneously detected only with a shifting factor detection error ($\xi \rightarrow \xi_{e,}$) where $\xi_e = 2$ while data symbols, TAP, and AAP are decoded correctly. In this case, the corresponding error event can be expressed as follows:

$$\mathbf{X} \rightarrow \hat{\mathbf{X}} = \begin{bmatrix} 0 & 0 & 0 \\ \breve{s}_1^R + j\breve{s}_3^I & 0 & 0 \\ 0 & \breve{s}_3^R + j\breve{s}_2^I & 0 \\ 0 & 0 & \breve{s}_2^R + j\breve{s}_1^I \end{bmatrix} \rightarrow \begin{bmatrix} 0 & 0 & 0 \\ \breve{s}_1^R + j\breve{s}_2^I & 0 & 0 \\ 0 & \breve{s}_3^R + j\breve{s}_1^I & 0 \\ 0 & 0 & \breve{s}_2^R + j\breve{s}_3^I \end{bmatrix}. \quad (10)$$

For this specific error event, different from single symbol errors, three non-zero elements occur in $\mathbf{A}$ due to the erroneous shift in the imaginary parts of data symbols. Here, $\mathrm{rank}(\mathbf{A}) = d_2 = 3$ is always obtained for this error event.

3) TAP Selection: The effect of TAP selection on diversity order is analyzed thirdly. Assume that the transmission matrix $\mathbf{X}$, with parameters $N_t = 4$, $\Omega = 3$, $\xi = 1$, $\mathbf{t} = [1,3,2]^{\mathrm{T}}$, $\mathbf{a} = [2,3,4]^{\mathrm{T}}$, $\tilde{\mathbf{s}} = [\tilde{s}_1, \tilde{s}_2, \tilde{s}_3]^{\mathrm{T}}$, is transmitted, and $\hat{\mathbf{X}}$ is erroneously detected only with a TAP error ($\mathbf{t} \rightarrow \mathbf{t}_e$) where $\mathbf{t}_e = [1,2,3]$ is erroneously detected while the shifting factor, data symbols, and AAP are decoded correctly. In this case, the error event can be expressed as follows:

$$\mathbf{X} \rightarrow \hat{\mathbf{X}} = \begin{bmatrix} 0 & 0 & 0 \\ \tilde{s}_1 & 0 & 0 \\ 0 & \tilde{s}_3 & 0 \\ 0 & 0 & \tilde{s}_2 \end{bmatrix} \rightarrow \begin{bmatrix} 0 & 0 & 0 \\ \tilde{s}_1 & 0 & 0 \\ 0 & \tilde{s}_2 & 0 \\ 0 & 0 & \tilde{s}_3 \end{bmatrix}. \quad (11)$$

For this specific error event, $\mathrm{rank}(\mathbf{A}) = d_3 = 2$ represents the diversity order. The error in TAP causes two non-zero elements, which are located in different rows and columns, in $\mathbf{A}$. Hence, A diversity order of 2 is warranted.

4) AAP Selection: The last step in our diversity analysis is the investigation of the effect of erroneous AAP detection on the diversity order. Assume that the transmission matrix $\mathbf{X}$, with parameters $N_t = 4$, $\Omega = 3$, $\xi = 1$, $\mathbf{t} = [1,3,2]^{\mathrm{T}}$, $\mathbf{a} = [2,3,4]^{\mathrm{T}}$, $\tilde{\mathbf{s}} = [\tilde{s}_1, \tilde{s}_2, \tilde{s}_3]^{\mathrm{T}}$, is transmitted, and $\hat{\mathbf{X}}$ is erroneously detected only with an AAP error ($\mathbf{a} \rightarrow \mathbf{a}_e$) while shifting factor, TAP, and data symbols are decoded correctly, and $\mathbf{a}_e = [3,4,1]$. In this case, the error event can be expressed as follows:

$$\mathbf{X} \rightarrow \hat{\mathbf{X}} = \begin{bmatrix} 0 & 0 & 0 \\ \tilde{s}_1 & 0 & 0 \\ 0 & \tilde{s}_3 & 0 \\ 0 & 0 & \tilde{s}_2 \end{bmatrix} \rightarrow \begin{bmatrix} 0 & 0 & \tilde{s}_2 \\ 0 & 0 & 0 \\ \tilde{s}_1 & 0 & 0 \\ 0 & \tilde{s}_3 & 0 \end{bmatrix}. \quad (12)$$

For this specific error event, the minimum diversity order of 2 is guaranteed with $\mathrm{rank}(\mathbf{A}) = d_4 \geq 2$.

As a result, all worst case error events are provided for different type of detection errors. Even for these worst case pairwise error events, our proposed scheme provides at least second order diversity. By induction, the other pairwise error events can be also investigated. Finally, in view of all the above, SM-SSD provides $\min_{\mathbf{X},\hat{\mathbf{X}}} \mathrm{rank}(\mathbf{A}) = 2$ which demonstrates that the diversity order of the system is 2.

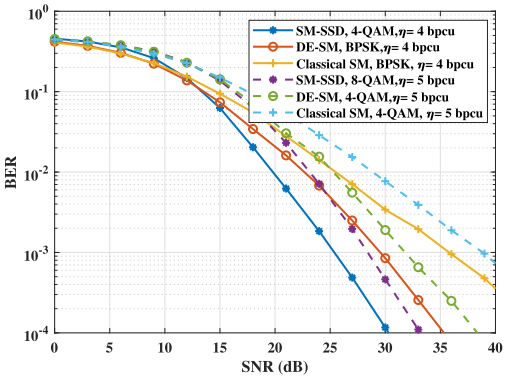

Fig. 2. BER performance comparison of SM-SSD with benchmark schemes for a 8×1 system under 4 and 5 bpcu.

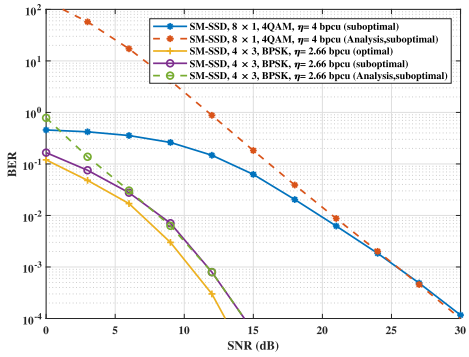

Fig. 3. BER performance comparison of SM-SSD with theoretical results for 8×1 sytem with 4 bpcu and 4×3 system with 2.66 bpcu, respectively.

IV. Simulation Results

In this section, Monte Carlo simulations are demonstrated to compare the BER performance of SM-SSD with classical SM and an improved SM scheme called diversity-enhanced SM (DE-SM). DE-SM processes two time slots jointly and interleaves the real and imaginary parts of data symbols. Then, DE-SM activates one transmit antenna in each time slot and transmits the interleaved data symbols respectively. The results are verified by theoretical upper bound derivations. In addition, the BER performance of SM-SSD is evaluated for the correlated and uncorrelated channels. Lastly, the variation of spectral efficiency is observed for different Ω and N_t values under the same modulation order.

Fig. 2 shows a BER performance comparison between SM-SSD for $\Omega = 3$ and the benchmark schemes under 4 and 5 bpcu for a 8×1 system. As seen from Fig. 2, SM-SSD has a higher diversity order than the benchmark schemes, and having higher diversity order results in better BER performance with respect to the benchmark schemes even though SM-SSD has a higher modulation order. At the BER level of 10^{-4}, SM-SSD provides at least 5 dB SNR gain with respect to the benchmark schemes under both data rates. Here, for a spectral efficiency of 4 bpcu, a total number of 4096 and

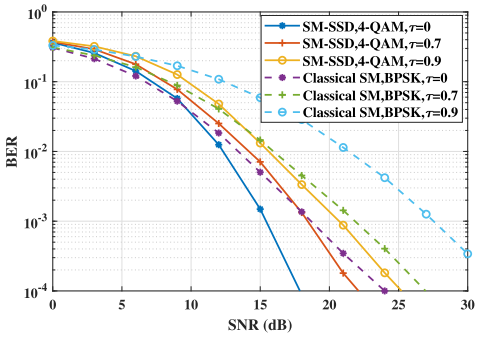

Fig. 4. BER performance comparison of SM-SSD for a 8×2 system under 4 bpcu for different τ values.

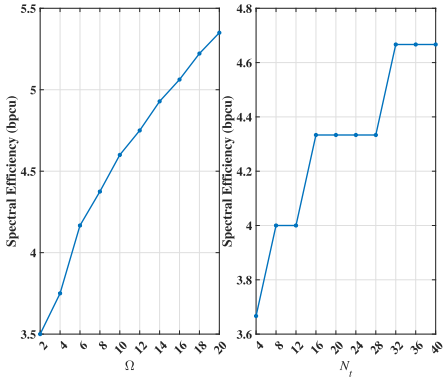

Fig. 5. Spectral efficiency variation of SM-SSD with respect to a) Ω with $N_T = 4$, b) N_t with $\Omega = 3$.

256 metric calculations are performed to decode SM-SSD and DE-SM signals, respectively. Hence, an interesting trade-off is provided between the error performance and decoding complexity.

Fig. 3 provides the error performance comparison between the theoretical BER upper bound and Monte Carlo simulations, with rotation angles obtained by optimal and suboptimal algorithms. SM-SSD with optimal rotation angles has 1 dB SNR gain over suboptimal case at 10^{-3} BER value. However, optimal rotation angles are obtained with an exhaustive search, which is not feasible for higher spectral efficiency values. As seen from Fig. 3, the theoretical upper bound and computer simulations match at high SNR values as expected. Note that theoretical analysis is also valid for all η values.

In Fig. 4, the BER performances of SM-SSD with 4-QAM and classical SM with BPSK are investigated for $\tau = 0$, 0.7, 0.9 under 4 bpcu. It is seen clearly that the increase in the channel correlation coefficient degrades the BER performances of both schemes, however, SM-SSD is stronger than classical SM against the channel correlation. Finally, Fig. 5 demonstrates the variation in spectral efficiency depending on the changes in Ω and N_t for M = 4.

In Fig. 5(a), the spectral efficiency changes with Ω while $N_t = 4$ and $M = 4$. The spectral efficiency increases with Ω proportionally since the number of possible TAPs and ξ increases when Ω increases. In addition, the spectral efficiency also increases with N_t as seen in Fig. 5(b). However, there is a loss in spectral efficiency with respect to the benchmark schemes due to the elimination of possible AAPs to prevent transmit diversity degradation. It is transparent that there is a trade-off between the transmit diversity and the spectral efficiency.

V. Conclusion

In this letter, a novel SM-based transmission scheme named SM-SSD has been proposed for MIMO systems. SM-SSD processes multiple time slots jointly. A clever shifting mechanism for the imaginary parts of data symbols is described to apply SSD. Besides, TAP and AAP selection algorithms are introduced for data transmission and diversity enhancement, respectively. Despite its high decoding complexity, SM-SSD provides an outstanding error performance. The design of a low-complexity detector for SM-SSD is left as future work.

References

[1] E. Basar, M. Wen, R. Mesleh, M. Di Renzo, Y. Xiao, and H. Haas, "Index modulation techniques for next-generation wireless networks," *IEEE Access*, vol. 5, pp. 16693–16746, 2017.

[2] E. Başar, "Index modulation techniques for 5G wireless networks," *IEEE Commun. Mag.*, vol. 54, no. 7, pp. 168–175, Jul. 2016.

[3] R. Mesleh, H. Haas, C. W. Ahn, and S. Yun, "Spatial modulation—A new low complexity spectral efficiency enhancing technique," in *Proc. 1st Int. Conf. Commun. Netw. China*, Oct. 2006, pp. 1–5.

[4] E. Başar, U. Aygolu, E. Panayirci, and H. V. Poor, "Space-time block coded spatial modulation," *IEEE Trans. Commun.*, vol. 59, no. 3, pp. 823–832, Mar. 2011.

[5] M. Di Renzo, H. Haas, A. Ghrayeb, S. Sugiura, and L. Hanzo, "Spatial modulation for generalized MIMO: Challenges, opportunities, and implementation," *Proc. IEEE*, vol. 102, no. 1, pp. 56–103, Jan. 2014.

[6] R. Mesleh, O. Hiari, and A. Younis, "Generalized space modulation techniques: Hardware design and considerations," *Phys. Commun.*, vol. 26, pp. 87–95, Feb. 2018.

[7] J. Wang, S. Jia, and J. Song, "Generalised spatial modulation system with multiple active transmit antennas and low complexity detection scheme," *IEEE Trans. Wireless Commun.*, vol. 11, no. 4, pp. 1605–1615, Apr. 2012.

[8] R. Mesleh, S. S. Ikki, and H. M. Aggoune, "Quadrature spatial modulation," *IEEE Trans. Veh. Technol.*, vol. 64, no. 6, pp. 2738–2742, Jun. 2014.

[9] R. Rajashekar, K. V. S. Hari, and L. Hanzo, "Antenna selection in spatial modulation systems," *IEEE Commun. Lett.*, vol. 17, no. 3, pp. 521–524, Mar. 2013.

[10] S. Alamouti, "A simple transmit diversity technique for wireless communications," *IEEE J. Sel. Areas Commun.*, vol. 16, no. 8, pp. 1451–1458, Oct. 1998.

[11] X. Li and L. Wang, "High rate space-time block coded spatial modulation with cyclic structure," *IEEE Commun. Lett.*, vol. 18, no. 4, pp. 532–535, Apr. 2014.

[12] C. Jeon and J. W. Lee, "Multi-strata space-time coded spatial modulation," *IEEE Commun. Lett.*, vol. 19, no. 11, pp. 1945–1948, Nov. 2015.

[13] J. Boutros and E. Viterbo, "Signal space diversity: A power- and bandwidth-efficient diversity technique for the Rayleigh fading channel," *IEEE Trans. Inf. Theory*, vol. 44, no. 4, pp. 1453–1467, Jul. 1998.

[14] S. Althunibat and R. Mesleh, "Enhancing spatial modulation system performance through signal space diversity," *IEEE Commun. Lett.*, vol. 22, no. 6, pp. 1136–1139, Jun. 2018.

[15] Y. Yang, P. Ma, K. Pang, Z. Bai, T. Han, and K. Kwak, "Design of space signal diversity based quadrature spatial modulation," in *Proc. 19th Int. Symp. Commun. Inf. Technol. (ISCIT)*, Sep. 2019, pp. 173–177.

[16] M. K. Simon and M.-S. Alouini, *Digital Communications over Fading Channels*. New York, NY, USA: Wiley, 2001.

[17] A. T. Dogukan, O. F. Tugtekin, and E. Basar, "Coordinate interleaved OFDM with power distribution index modulation," *IEEE Commun. Lett.*, vol. 26, no. 8, pp. 1908-1912, Aug. 2022.

[18] A. Paulraj, A. P. Rohit, R. Nabar, and D. Gore, *Introduction to Space-Time Wireless Communications*. Cambridge, U.K.: Cambridge Univ. Press, 2003.